Contrib Mineral Petrol (2007) 154:619–633
DOI 10.1007/s00410-007-0217-5

ORIGINAL PAPER

Postcumulus processes in oceanic-type olivine-rich cumulates: the role of trapped melt crystallization versus melt/rock interaction

G. Borghini · E. Rampone

Received: 14 November 2006 / Accepted: 4 May 2007 / Published online: 31 May 2007

Abstract Combined microstructural and geochemical investigations on MORB-type primitive olivine-rich cumulates intruded in the Erro–Tobbio (ET) mantle peridotites (Voltri Massif, Ligurian Alps, Italy) revealed that significant chemical changes in minerals were caused by postcumulus crystallization. This is indicated by the occurrence of accessory interstitial minerals (Ti-pargasite, orthopyroxene and Fe–Ti oxides) and by systematic chemical zoning in intercumulus clinopyroxene, resulting in marked trace element (e.g. REE, Ti and Zr) enrichment at constant high Mg-numbers (0.88–0.91) and LREE depletion. Geochemical modelling shows that low trapped melt amounts (<5%) are sufficient to produce the observed trace element enrichments. Chemical zoning in large (mm-size) clinopyroxenes was dominantly caused by in situ fractional crystallization of trapped interstitial liquid rather then porous flow migration of externally derived evolved melts. Zr enrichment relative to REEs in vermicular clinopyroxene and pargasitic amphibole point to small-scale migration and interaction between residual evolved low melt fractions and the olivine cumulus matrix at final stage of crystallization.

Communicated by J. Hoefs.

Electronic supplementary material The online version of this article (doi:10.1007/s00410-007-0217-5) contains supplementary material, which is available to authorized users.

G. Borghini (✉) · E. Rampone
Dipartimento per lo Studio del Territorio e delle sue Risorse, Università degli Studi di Genova, Corso Europa 26, 16132 Genova, Italy
e-mail: giulio.borghini@unige.it

Keywords Olivine cumulates · Trapped melt · Melt/rock interaction · In situ trace element analyses

Introduction

Postcumulus processes have been widely described in cumulates from continental layered intrusions and plutons (Barnes 1986; Cawthorn et al. 1992; Cawthorn 1996; Bedard 1994, 2001; Claeson and Meurer 2004; Charlier et al. 2005; Bernstein 2006) and oceanic environments (Meyer et al. 1989; Natland et al. 1991; Ross and Elthon 1997; Tribuzio et al. 1999; Gillis and Meyer 2001; Natland and Dick 2001; Coogan et al. 2000a, b; Gao et al. 2007). These studies have shown that the crystallization of interstitial melt trapped within the cumulus matrix plays an important role in the final mineral composition of cumulate rocks. The postcumulus crystallization of evolved interstitial melt has been also invoked to explain the occurrence of amphibole (and minerals such as Fe–Ti oxides and apatite) within rather primitive oceanic and ophiolitic MORB-type cumulates (Natland et al. 1991; Gillis 1996; Tribuzio et al. 1999, 2000; Gillis and Meyer 2001; Coogan et al. 2001). A matter of debate is whether these processes can be entirely accounted by interaction between cumulus minerals and variable amounts of evolved interstitial liquid produced by in situ fractional crystallization of indigenous trapped melt, i.e. a ‘‘closed system’’ crystallization process (Barnes 1986; Meyer et al. 1989; Chalokwu and Grant 1990; Bedard 1994; Cawthorn 1996; Gillis and Meyer 2001; Charlier et al. 2005; Bernstein 2006), or they require an exotic component, i.e. the migration of externally derived evolved melts (Natland et al. 1991; Mathez 1995; Ross and Elthon 1997; Tribuzio et al. 1999, 2000; Natland

and Dick 2001; Coogan et al. 2000b; Meurer and Claeson 2002; Gao et al. 2007).

Geochemical models (Bedard 1994; Cawthorn 1996; Charlier et al. 2005) have revealed that intercumulus minerals crystallized from trapped interstitial melt may have very high REE concentrations, without needing to invoke infiltration metasomatism by an external liquid enriched in incompatible elements. On the other hand, fractional crystallization combined with simultaneous metasomatism between cumulate crystals and migrating porous melt has been documented in both layered intrusions and oceanic gabbros (Natland et al. 1991; Mathez 1995; Natland and Dick 2001; Coogan et al. 2000b; Gao et al. 2007). This process, named synkinematic differentiation or differentiation by deformation, has been invoked to explain trace element zoning and chromatographic fractionation in minerals (Coogan et al. 2000b; Gao et al. 2007), and is inferred to play an important role in the magmatic evolution of the oceanic crust at slow-spreading ridges (Natland and Dick 2001; Gao et al. 2007).

Although a large number of papers have been devoted to studies of postcumulus crystallization effects in cumulate rocks (especially in layered intrusions), a few works have yet documented chemical variations in cumulus and postcumulus phases by detailed in situ major and trace element mineral analyses in different microstructural sites (e.g. Ross and Elthon 1997; Tribuzio et al. 1999; Coogan et al. 2000a, b; Meurer and Claeson 2002; Gao et al. 2007; Bernstein 2006). In this paper, we present combined microstructural and in situ trace element mineral chemistry investigations on MORB-type olivine cumulates intruded in the ET mantle peridotites (Voltri Massif). The studied samples pertain to a hectometre-scale stratified cumulate body, showing gradational contacts with the host mantle peridotites, and crosscut by later olivine gabbro lenses and dikes (Borghini et al. 2007). The cumulate body is mostly dominated by cpx–bearing troctolites (plus minor plag–cpx–bearing dunites and plag–bearing wehrlites). According to Borghini et al. (2007), they represent cumulus products crystallized from rather primitive N-MORB-type melts similar to oceanic gabbroic rocks from slow spreading settings. These rocks record significant trace element chemical zoning in intercumulus minerals (particularly clinopyroxene) and contain rare and diffuse interstitial pargasitic amphibole associated to interstitial clinopyroxene ± Fe–Ti oxides. The major aim of this work is therefore to document, by means of bulk-rock and in situ major and trace element mineral analyses, the chemical and textural effects of postcumulus processes in MORB-type olivine-rich cumulates, and to discuss the origin of related interstitial melts in the context of closed versus open system crystallization.

Samples and analytical methods

Troctolites have medium to coarse grain size and consist of euhedral cumulus olivine (72–80 wt.%), interstitial plagioclase (17–24 wt.%) and subordinate poikilitic clinopyroxene (2–4 wt.%) (eTable 1, Fig. 1a, b). Clinopyroxene is present in coarse mm-sized anhedral grains (Fig. 1a) and in thin (<400 μm) interstitial crystals (Fig. 1b–d). These latters occur as rims between olivine and plagioclase or between olivine grains, and in places are in optical continuity with larger clinopyroxene crystals (Fig. 1a); they often show lobate contacts against cumulus olivine, indicative of partial olivine resorption (Fig. 1b, c). Small euhedral chromite crystals (about 1% by volume) are commonly found within plagioclase. In all samples, plagioclase is partly replaced by low-grade alteration products.

Brown amphibole, Fe–Ti oxides and orthopyroxene (associated with vermicular clinopyroxene or as discontinuous rim around olivine) occur as small interstitial accessory minerals. Amphibole crystallizes as thin rims (usually <60 μm) mostly confined around chromite grains or in thin vermicular grains between olivine and plagioclase locally associated with vermicular clinopyroxene (Fig. 1d). It is present in very low amounts in all samples (<1% by vol.), and it is more diffuse in samples MF8 and MF51. Small rims (≈5–10 μm) of Fe–Ti oxides (mostly ilmenite) have been observed by X-R mapping between chromite grain and amphibole rims.

Major and trace element bulk-rock compositions of three selected troctolite samples are reported in eTable 1. Troctolites have high Mg-numbers (0.89–0.90) and display very low contents of incompatible elements like Y (1.01–1.65 ppm) and Zr (3.25–4.77 ppm). They exhibit overall low REE concentrations (M- to H-REE contents below $2 \times C1$), flat to slightly LREE-depleted patterns ($Ce_N/Sm_N = 0.82–1.05$) and positive Eu anomalies ($Eu_N/Eu_N^* = 1.75–2.42$) (Fig. 2). All these features indicate that the bulk rock compositions are mostly controlled by the relative proportions of the cumulate minerals, i.e. higher modal plagioclase and olivine with respect to clinopyroxene.

Whole-rock major element analyses were performed by XRF technique at the Dipartimento di Scienze della Terra, Università di Modena. The bulk trace element data were determined on a quadrupole VG-PG2 Inductively Coupled Plasma-Mass Spectometry (ICP-MS) at ISTEEM (Université de Montpellier 2, France) following the procedure described by Ionov et al. (1992). REE, Sr, Zr, Hf, Rb and Ba concentrations were determined by external calibration. Detailed description of the method and detection limits can be found in Godard et al. (2000). Major element mineral chemistry data were obtained (1) at the Dipartimento per lo studio del Territorio e delle sue Risorse, University of

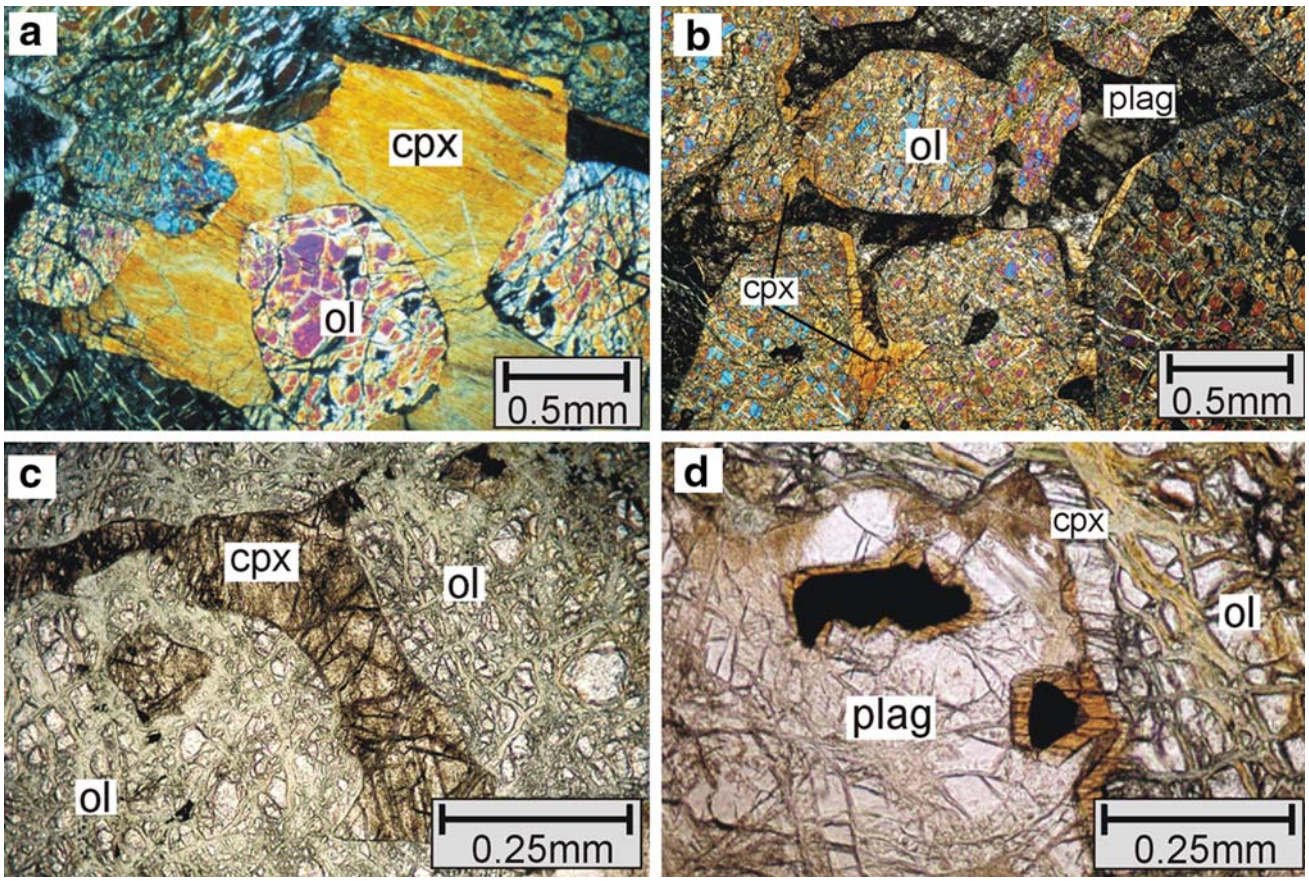

Fig. 1 Textural features of the ET troctolites. **a** Coarse mm-size anhedral clinopyroxene (*cpx*) between rounded cumulus olivines (*ol*) (*crossed nicols*). **b** Thin ''vermicular'' clinopyroxene (*cpx*) between cumulus olivine and anhedral plagioclase (*plag*) (*crossed nicols*). **c** Interstitial clinopyroxene (*cpx*) showing lobate contacts against cumulus olivine (*ol*) (*uncrossed nicols*). **d** Rim of brown Ti-rich pargasitic amphibole (*amph*) around chromite grains; vermicular amphibole and clinopyroxene between plagioclase and olivine (*uncrossed nicols*)

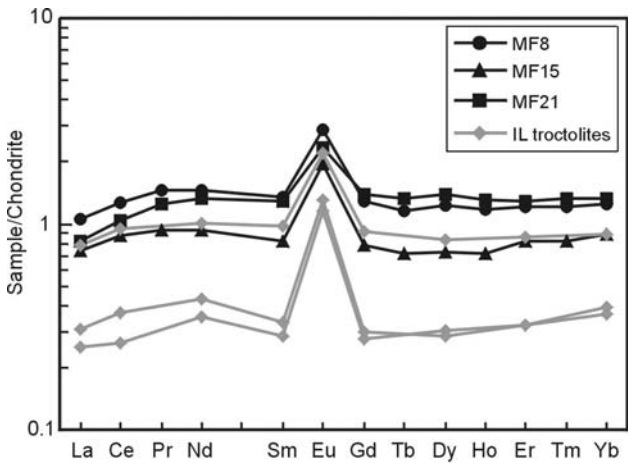

Fig. 2 Chondrite-normalized whole-rock REE abundances of the ET troctolites. The *grey* REE spectra refer to the Internal Liguride ophiolitic troctolites (data from Rampone et al. 1998). Normalization factor from Anders and Ebihara (1982)

Genova, by a Philips SEM 515 electron microscope equipped with an X-ray dispersive analyser energy dispersive spectrometer (EDS) (accelerating potential 15 kV; sample current 20 nA), and (2) at the C.N.R.- Centro di studio per la Minerogenesi e la Geochimica applicata of Firenze by a JEOL JXA-8600 electron microscope, equipped with four wavelength dispersive spectrometers (WDS) and one EDS (accelerating potential 15 kV; sample current 10 nA) (Vaggelli et al. 1999). In situ trace element mineral analyses were carried out by LAM-ICP-MS techniques at IGG-CNR (Istituto di Geoscienze e Georisorse) in Pavia. A detailed description of this analytical procedure is reported in Tiepolo et al. (2003). Mineral REE abundances were normalized to the average C1 chondrite composition (Anders and Ebihara 1982).

In order to trace the chemical variations related to postcumulus crystallization, in situ analyses were performed in clinopyroxene grains of different sizes and in different microtextural occurrences: (1) core (C), interme-

diate (I) and rim (R) (<50 μm inward from the crystal rim) traverses in larger grains (1–2 mm), (2) small interstitial grains (Int) (width ranging 100–400 μm) and (3) thin vermicular grains (V) (width lower than 100 μm). In plagioclase, diffuse low-grade alteration has limited detailed core–rim analytical investigations, especially for the trace elements.

Mineral composition

Representative major and trace element mineral compositions are reported in eTables 2–4. Olivine displays homogeneous compositions, mostly Fo_{88}–Fo_{89}. Spinels have high Cr concentrations (Cr# = 0.51–0.60) and rather high and variable Ti contents (TiO_2 = 1.06–2.60 wt.%); no systematic core–rim variations have been documented, although a Ti decrease is observed in some spinel rims associated to Fe–Ti oxides.

As documented in Borghini et al. (2007), clinopyroxenes in the troctolites show major element concentrations consistent with those of clinopyroxenes from the most primitive oceanic cumulates (Elthon et al. 1992). They also display remarkable compositional variations systematically correlated with microstructural site, i.e. TiO_2 increase and Cr_2O_3 decrease from cores to rims of larger crystals, to interstitial and vermicular grains, at rather high and constant Mg# (0.88–0.91) (Fig. 3). In Fig. 3a, we have reported for comparison: (1) the compositional field of oceanic cumulates (Elthon et al. 1992) and (2) the cumulus and postcumulus trends documented in oceanic (Ross and Elthon 1997; Meyer et al. 1989) and ophiolitic (Tribuzio et al. 1999) olivine gabbros. It is remarkable that clinopyroxenes in the studied samples define a steeper trend, characterized by a significant TiO_2 enrichment (up to 1.45 wt.%) coupled to a narrow Mg# variation.

Clinopyroxene cores are characterized by LREE (light earth rare elements) depletion (La_N/Sm_N = 0.12–0.16), nearly flat middle (M-) to heavy (H-) REE concentrations (at about 10–15 × C1) and slight to almost absent negative Eu anomaly (Eu_N/Eu_N^* = 0.91–0.99) (Fig. 4a). In terms of M- to H-REE, they resemble calculated compositions of clinopyroxene in equilibrium with average MORB (Fig. 4a), although displaying slightly higher LREE abundances. Clinopyroxenes exhibit an overall progressive enrichment in REE absolute concentrations, coupled to the development of strong negative Eu anomalies, from cores to rims of large crystals, to interstitial and vermicular grains (Fig. 4a). This is also documented in Fig. 5, which shows the REE clinopyroxene compositions in core–intermediate–rim profiles and interstitial grains from samples MF21 and MF8. Vermicular grains have the highest M- to H-REE concentrations (up to 40–50 × C1),

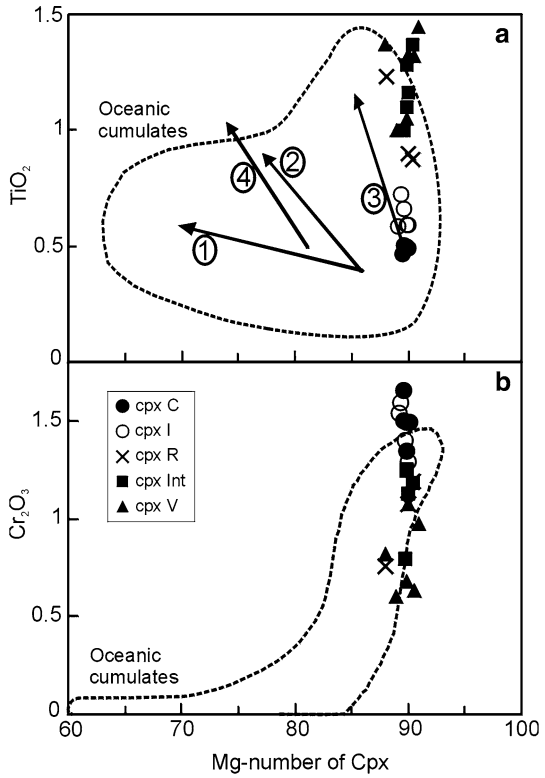

Fig. 3 **a** TiO_2 contents versus Mg# values [100 × Mg/(Mg + Fe)] in clinopyroxenes from the ET troctolites. (*C*), (*I*), (*R*) refer to core–intermediate–rim profiles of large (mm-size) clinopyroxene grains; (Int) and (V) refer to interstitial (<400 μm) and vermicular (<100 μm) clinopyroxene grains. The field refers to the composition of clinopyroxenes in oceanic cumulates (data from Elthon et al. 1992). The *arrows* describe different crystallization trends; *arrows* (1) and (2): cumulus and postcumulus crystallization trends, respectively, in Leg 153 gabbroic rocks (Ross and Elthon 1997); *arrow* (3): postcumulus trend in cumulate gabbros from the Southwest Indian Ridge (Meyer et al. 1989); *arrow* (4): postcumulus trend in Northern Apennine ophiolitic olivine gabbros (Tribuzio et al. 1999). **b** Cr_2O_3 contents versus Mg# values [100 × Mg/(Mg + Fe)] in ET clinopyroxenes. The field refers to the composition of clinopyroxenes from oceanic cumulates (from Elthon et al. 1992)

and pronounced negative Eu anomalies (Eu_N/Eu_N^* = 0.33–0.64), although preserving the same LREE fractionation (La_N/Sm_N = 0.09–0.11) (Fig. 4a).

Another remarkable geochemical feature is shown by Ti and Zr behaviour. Large clinopyroxene crystals (from cores to rims) display negative Zr (Zr_N/Zr_N^* = 0.31–0.63) and Ti (Ti_N/Ti_N^* = 0.40–0.69) anomalies. By contrast the interstitial and vermicular grains, although preserving Ti depletion (Ti_N/Ti_N^* = 0.34–0.66), exhibit a progressive increase in Zr relative to the adjacent REE, resulting in positive Zr anomalies (Zr_N/Zr_N^* = 0.77–1.92) (Fig. 6a). The Sr contents are invariably low in all clinopyroxenes (Sr = 11–17.6 ppm), resulting in marked negative Sr anomalies (Fig. 6a).

Plagioclases have An_{58}–An_{66}. No systematic core–rim compositional variations are detected, although lower An

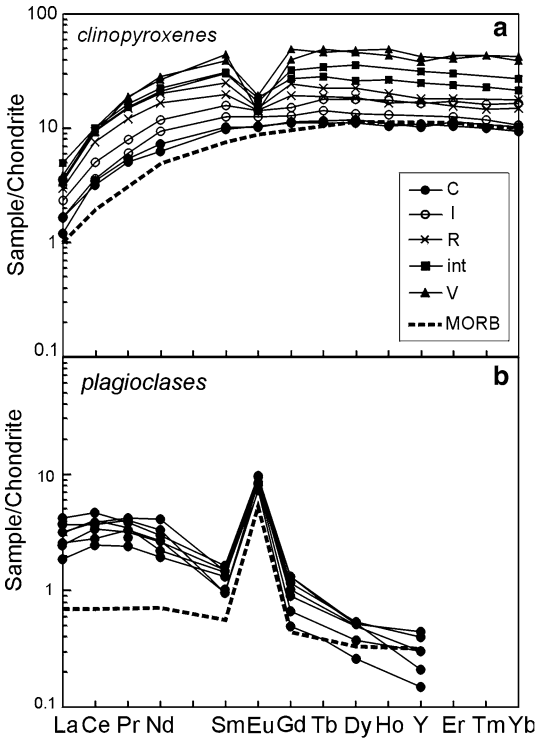

Fig. 4 Chondrite-normalized REE abundances of selected clinopyroxenes (**a**) and plagioclase (**b**) from the ET troctolites. Computed REE concentrations in clinopyroxene (**a**) and plagioclase (**b**) in equilibrium with average N-MORB (from Hofmann 1988; D_{REE} in clinopyroxene from Suhr et al. 1998) are also shown (*dashed* spectra). Normalization factors as in Fig. 2. Symbols as in Fig. 3

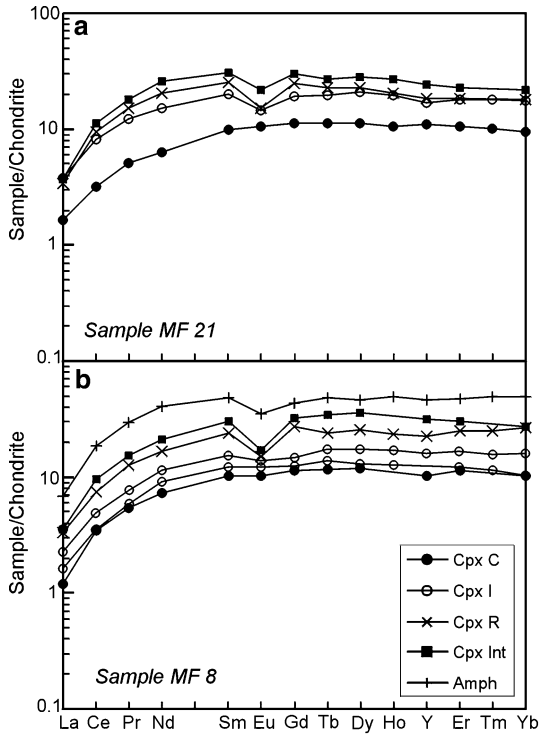

Fig. 5 **a** Chondrite-normalized REE abundances of representative core–intermediate–rim large grain profile and interstitial grains of clinopyroxenes from sample MF21. **b** Chondrite-normalized REE abundances of representative core–intermediate–rim profile of large clinopyroxene, interstitial clinopyroxene and amphibole from sample MF8. Normalization factors as in Fig. 2. Symbols as in Fig. 3

contents are often observed towards the rims of single crystals. Plagioclases REE spectra are characterized by constant decrease from LREE to HREE (La_N/Sm_N = 1.38–3.89) and marked positive Eu anomalies (Eu_N/Eu_N^* = 6.6–10.2). As shown in Fig. 4b, they display overall higher LREE concentrations (up to 3–4 × C1) with respect to the composition of computed plagioclase in equilibrium with an average MORB. Data reported in eTable 3 and Fig. 4b refer to the compositions of crystal cores. In a few larger grains, core–rim analyses have been performed, and no systematic trace element zonation has been observed.

Amphiboles are mostly pargasites to pargasitic hornblendes (according to Leake classification 1997), with relatively high-Mg values (Mg# = 0.86–0.89) and Ti content (TiO_2 = 3.17–4.06 wt.%). They display LREE-depleted REE spectra (La_N/Sm_N = 0.11–0.15) with negative Eu anomalies (Eu_N/Eu_N^* = 0.61–0.77), similar in shape to those of clinopyroxenes at higher concentrations (up to 50–60 × C1) (Figs. 5b, 6b). The trace element compositions of amphiboles in the ET troctolites are compared, in Fig. 6b, with interstitial amphiboles in the Northern Apennine olivine gabbros (Tribuzio et al. 2000); noteworthy ET amphiboles exhibit much lower Nb, LREE and Zr concentrations, although having similar low Ba, K and Sr (52.9–89.4 ppm) abundances.

Discussion

Textural and chemical evidence of postcumulus crystallization

The postcumulus interstitial liquid crystallization in the troctolites is indicated by the occurrence of: (1) accessory interstitial minerals (as amphibole, orthopyroxene and Fe–Ti oxides), which are not in textural and chemical equilibrium with cumulus olivine and cores of plagioclase and clinopyroxene, (2) systematic chemical zoning of clinopyroxene in different microstructural sites (coarse anhedral crystals versus thin vermicular grains), (3) low anorthite and high LREE contents in plagioclase.

The crystallization of evolved mineral phases in primitive cumulates (troctolites and olivine gabbros) has been previously documented in both oceanic and ophiolitic settings. Tribuzio et al. (1999) reported the occurrence of minor orthopyroxene, Fe–Ti oxides, brown

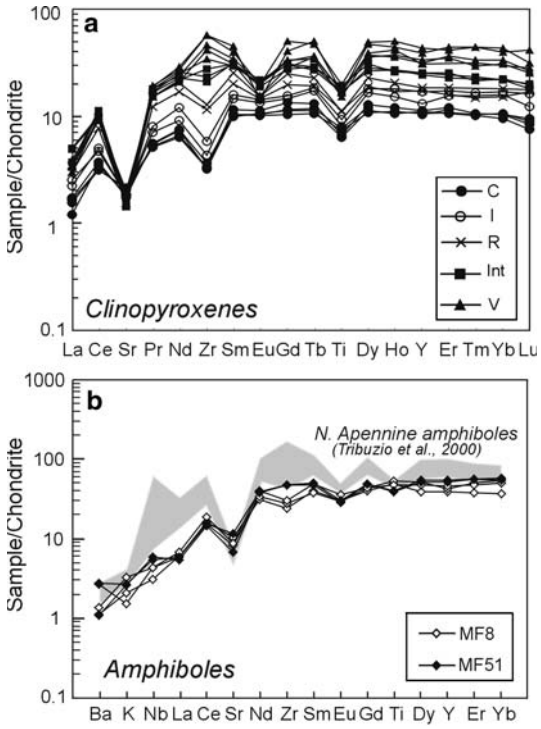

Fig. 6 **a** Chondrite-normalized spiderdiagrams of selected clinopyroxenes. Symbols as in Fig. 3. **b** Chondrite-normalized spiderdiagrams of amphiboles. The *grey field* refers to the amphiboles in Northern Apennine olivine-bearing gabbros (Tribuzio et al. 2000). Normalization factors as in Fig. 2

amphibole and apatite in olivine-bearing gabbros from the Northern Apennine ophiolites, whereas accessory zirconia and sulfide minerals have been documented in oceanic olivine gabbros (Ross and Elthon 1997). Such textural features are commonly associated to trace element enrichment of intercumulus and cumulus minerals, and have been interpreted as resulting by late-stage crystallization of interstitial melts (Bedard 1994; Cawthorn 1996; Ross and Elthon 1997; Tribuzio et al. 1999; Charlier et al. 2005; Bernstein 2006). As described by Barnes (1986), the solidification of trapped intercumulus liquid in orthocumulates is a process leading to both postcumulus overgrowths on cumulus crystals and late crystallization of additional interstitial minerals enriched in component excluded from the cumulus phases. Specifically, postcumulus crystal overgrowth can result in marked chemical zoning of mineral phases (Tribuzio et al. 1999; Ross and Elthon 1997; Coogan et al. 2000a, b; Gao et al. 2007; Bernstein 2006), or in complete re-equilibration of minerals (with significant enrichment of many incompatible elements) by subsequent diffusion (Barnes 1986; Meyer et al. 1989; Bedard 1994; Charlier et al. 2005).

In the ET troctolites, the main compositional evidence of postcumulus crystallization is the systematic chemical zoning in clinopyroxene related to its textural occurrence; such compositional variation consists of marked incompatible trace element enrichment (e.g. Ti, Zr and REE) coupled with compatible elements decrease (e.g. Cr) at constant high Mg-numbers (Mg# = 88–91), from cores to rims of larger crystals, to interstitial and vermicular grains (Figs. 3, 4a, 6a). These chemical features are evident in the Mg# versus TiO_2 diagram of Fig. 3a, where clinopyroxene compositions are compared with postcumulus trends documented in oceanic (Meyer et al. 1989; Ross and Elthon 1997) and ophiolitic (Tribuzio et al. 1999) olivine cumulates. These trends are quite different from a typical differentiation trend characterized by Ti increase at progressively lower Mg-numbers. The Mg#–TiO_2 trend defined by ET clinopyroxenes is much steeper than the postcumulus trends previously documented in oceanic and ophiolitic cumulates. The strong incompatibile element enrichment in vermicular clinopyroxene at constant Mg# is likely explained by the high modal contents of olivine (72–80 wt.%), relative to clinopyroxene (2–4 wt.%, eTable 1). As described by Barnes (1986) and Meyer et al. (1989), an olivine-rich cumulate matrix is able to buffer the major element composition (e.g. the Mg-number) of the intercumulus melt, but it cannot host most incompatible elements (e.g. Ti and REE), which are thus concentrated in the evolving interstitial melt. Mafic minerals (e.g. clinopyroxene and amphibole) crystallizing from the intercumulus melt will thus acquire ''decoupled'' compositional features, i.e. primitive Mg# coupled with incompatible element enrichment; this effect will be stronger at lower trapped melt volumes.

Postcumulus crystallization in the troctolites is also indicated by ''anomalous'' compositional features in plagioclase. Anorthite contents are variable, mostly An_{58}–An_{66}. Such values are lower than expected for plagioclase in equilibrium with olivine $Fo_{88–89}$. Bender et al. (1978) documented high anorthite contents (An $\approx$ 80) in plagioclase crystallizing from the FAMOUS basalts at moderate pressurs, and experimental studies on low pressure peridotite partial melting have inferred that plagioclase coexisting with liquid + lherzolite at 1 GPa is An_{75} (Walter and Presnall 1994; Green et al. 2001). This suggests that plagioclase in the ET troctolites equilibrated with a variably evolved intercumulus melt during crystallization, and it is consistent with the rather high LREE concentrations in plagioclase (up to 3–4 $\times$ C1), relative to the inferred composition of plagioclase in equilibrium with an average MORB (Fig. 4b).

It is remarkable that plagioclase, although displaying overall more ''evolved'' (anorthite-poor and LREE-enriched) compositions than expected in primitive MORB-type cumulates, has not preserved the systematic chemical zoning observed in clinopyroxene. This could be due to different diffusivity rates, especially for the LREE,

between plagioclase and clinopyroxene. A recent study on REE diffusion coefficients in clinopyroxene (Van Orman et al. 2001) has documented that overall REE mobility in clinopyroxene is low enough to preserve chemical zoning in clinopyroxene phenocrysts under natural conditions of basalt crystallization. On the other hand, Cherniak (2003) measured REE diffusion coefficients in different plagioclase compositions, and found that LREE diffuse two-order of magnitude faster in labradorite than in diopside. Thus, at similar time-temperature conditions, clinopyroxene is the likely mineral to preserve REE chemical zoning; this could explain the decoupled behaviour of plagioclase and clinopyroxene observed in the ET troctolites.

In summary, textural and chemical features of intercumulus minerals indicate that they crystallized from an evolved interstitial melt. We will show in the following section that the origin of such evolved melt was dominantly controlled by a process of in situ, closed-system fractional crystallization of small amounts of trapped intercumulus melt.

In situ trapped melt crystallization: constraints from the REE

The origin of evolved intercumulus liquid in primitive cumulates has been variably attributed to in situ fractional crystallization of indigenous melts or to porous flow migration of ''exotic'' liquids. Insights into these processes can result by coupled trace element bulk-rock and detailed in situ mineral investigations. Ross and Elthon (1997) inferred from REE mass balance calculations that HREE-enriched material was added to the cumulus matrix in LEG 153 gabbroic rocks. Tribuzio et al. (1999) argued, on the basis of LREE/HREE fractionation changes in clinopyroxenes from Northern Apennine olivine gabbros, that migration of an exotic component, rather than in situ trapped melt crystallization, was involved in the postcumulus process. Furthermore, recent papers inferred that reactive porous flow migration of melts within a crystal mush is the most likely process to explain HFSE/REE fractionation coupled to decreasing Mg# observed in core–rim profiles of clinopyroxenes from oceanic gabbros (Coogan et al. 2000b; Gao et al. 2007).

Tribuzio et al. (1999) invoked an exotic component by the observation that clinopyroxene rims and interstitial amphiboles have systematically higher La_N/Sm_N than the clinopyroxene cores (Fig. 7), and amphiboles also exhibit very high REE absolute concentrations (up to 80–100 × C1) and lower Mg# values (Mg# ≈ 73) relative to clinopyroxenes (Mg# = 76–82). On this basis, they concluded that the interstitial liquid was an LREE-enriched evolved exotic agent. Clinopyroxenes in the ET troctolites, in spite of marked chemical zoning from core to rim of

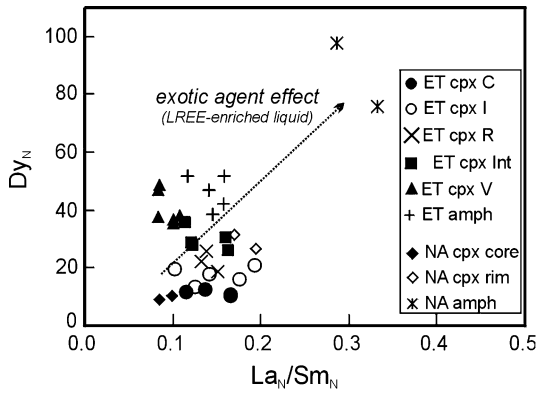

Fig. 7 Dy_N versus La_N/Sm_N variation in clinopyroxenes and amphiboles from the ET troctolites. Symbols as in Fig. 3. Also shown are the compositions of clinopyroxenes and amphiboles from the Northern Apennine (*NA*) olivine gabbros (data from Tribuzio et al. 1999, 2000)

large crystals, to interstitial and vermicular grains, are characterized by almost constant Mg# (0.88–0.91) and similar LREE fractionation (La_N/Sm_N = 0.09–0.17; Fig. 7). Also, unlike the data in Tribuzio et al. (1999), interstitial amphiboles in the ET troctolites exhibit quite similar LREE depletion (La_N/Sm_N = 0.11–0.15) at slightly higher absolute concentrations, relative to vermicular clinopyroxenes (Figs. 5, 7), and they preserve high-Mg values (Mg# = 86–88). These chemical characteristics argue against significant infiltration of exotic highly evolved melts, rather they suggest that postcumulus crystallization in the ET troctolites was dominantly controlled by closed-system trapped melt fractionation. Geochemical models have been developed to reproduce mineral compositional variations induced by the closed-system crystallization of trapped intercumulus liquids within a cumulate matrix (Bedard 1994; Cawthorn 1996) and to estimate the composition of primary liquids in equilibrium with cumulus minerals. Bedard (1994), proposed a mass balance model Equilibrium Distribution Method (EDM) assuming that, during postcumulus crystallization, the assemblage of ''cumulus mineral + some trapped melt'' (this latter inferred to be initially in equilibrium with the cumulus minerals) acts as a closed system. A useful application of the EDM method is that, if the composition of liquid in equilibrium with cumulates is known, it is possible to constrain the trapped melt fraction (TMF).

We have thus applied the Bedard's method to estimate the TMF crystallized within the cumulus matrix and to check whether the observed mineral compositional variations are consistent with a closed-system trapped melt crystallization. Modelling results for troctolite MF21 are shown in Fig. 8, where we report the REE patterns of clinopyroxene calculated assuming various amounts of TMF (0, 2, 5 and 7%) (see caption of Fig. 8 for more

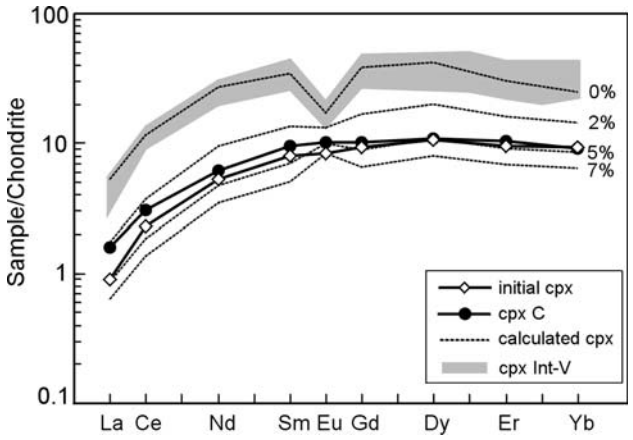

Fig. 8 Chondrite-normalized REE abundances of clinopyroxenes calculated with the EDM method (Equilibrium Distribution Method; from Bedard 1994) assuming TMFs of 0, 2, 5 and 7%. We used whole-rock REE abundances and modal composition of sample MF21 (see eTable 1), and trace element crystal/liquid partition coefficients from Suhr et al. (1998). Trapped melt modes have been assumed in order to account for the bulk-rock modal composition (eTable 1): cpx : plag = 0.5:0.5 for TMF = 2%, cpx : plag = 0.4:0.6 for TMF = 5%, cpx : plag = 0.3:0.7 for TMF = 7%. ''Initial cpx'' refers to the representative REE pattern of clinoyroxene in equilibrium with the potential liquid entrapped in the troctolites (*see text for explanation*). Representative REE abundances of clinopyroxene core in sample MF21 and the overall variation range defined by interstitial and vermicular clinopyroxenes (*grey field*) are also reported for comparison. Normalization factors as in Fig. 2

details). Computed clinopyroxene compositions are compared with those of clinopyroxene core in sample MF21 and the overall variation range defined by interstitial and vermicular clinopyroxenes. Also reported is the representative REE pattern of clinopyroxene cores in olivine gabbros associated with the troctolites, which is considered to reflect the composition of the cumulate parental liquid (Borghini et al. 2007). In other words, we assume that the composition of the liquid in equilibrium with the gabbro clinopyroxene reasonably represents the initial composition of potential liquid entrapped in the troctolites (''initial cpx'' in Fig. 8). The composition of calculated clinopyroxene is extremely sensitive to the TMF, and REE enrichment in clinopyroxene tends to decrease at increasing amount of trapped melt. Moreover, it is remarkable that the REE spectra of clinopyroxene computed assuming 5% of TMF is very similar to that of clinopyroxene in equilibrium with the parental liquid (initial cpx). This indicates that a small (<5%) TMF amount is sufficient to remove the trapped melt effect. Similar calculations were done for sample MF8 and MF15 and we obtained consistent results (TMF estimate ranging 3–5%). A low TMF amount is also suggested by the low modal clinopyroxene in the troctolites (2–4%) and by the evidence that the cores of larger poikilitic clinopyroxene grains still record REE concentrations resembling those of the ''initial cpx'' (Fig. 8). This indicates that clinopyroxene cores in the ET troctolites begin to crystallize when the trapped melt is not yet significantly evolved. Small amounts of trapped melt are also consistent with the lack of a significant compositional shift in the Mg-number of olivine, as described by Barnes (1986). Further evidence of low TMF is provided by estimates of the residual melt porosity (RMP) (according to the procedure and parameters proposed by Natland et al. 1991), which yielded percentage of final interstitial melt ranging 2–3 wt.%.

The EDM model also shows that clinopyroxene calculated assuming TMF = 0%, i.e. using the real bulk-rock mode and without removing the trapped melt effect, has absolute REE concentrations comparable to those of less enriched vermicular clinopyroxenes. Computed clinopyroxene at TMF = 0 represents the hypothetical ''average'' composition of clinopyroxene (modified by trapped melt), that would be observed in case of complete re-equilibration by subsequent diffusion. In contrast, we observed that clinopyroxene preserves a systematic chemical zoning: this points to progressive evolution of the interstitial trapped melt, according to a process of ''in situ'' fractional crystallization by incomplete mineral-liquid chemical reaction. A similar process has been inferred by Meurer and Claeson (2002) to explain the chemical heterogeneity of amphibole oikocrysts in arc-related cumulates.

To simulate the ''in situ fractionation'' of TMF, we performed a simplified model, which assumes various steps of equilibrium crystallization starting from a liquid in equilibrium with the ''initial cpx'' of Fig. 8, and changing the initial melt composition in each step. The fundamental assumption is that, as expected in a closed-system crystallization process, there is chemical exchange between liquid and crystallizing phases during the single steps of trapped melt crystallization, but such exchange was overall incomplete, thus causing interstitial melt fractionation and chemical zoning in clinopyroxene. The progressive TMF fractionation can be checked calculating trace element concentrations of clinopyroxene in equilibrium with the final residual liquid in each crystallization step, and using this latter as starting liquid in the following step. In each step, we arbitrarily fixed the remaining liquid fraction F and the proportion of crystallizing minerals, in order to account for the observed modal amounts of interstitial phases (see caption of Fig. 9 for modelling details). We thus assumed that 5% of trapped melt is definitely entrapped within the [cumulus olivine + interstitial plagioclase] framework, and that such TMF is initially in equilibrium with the mineral matrix. The 5% TMF crystallizes in four steps up to 90% crystallization and the overall crystallized solid is constituted by 70% clinopyroxene and 30% plagioclase. This implies about 3% clin-

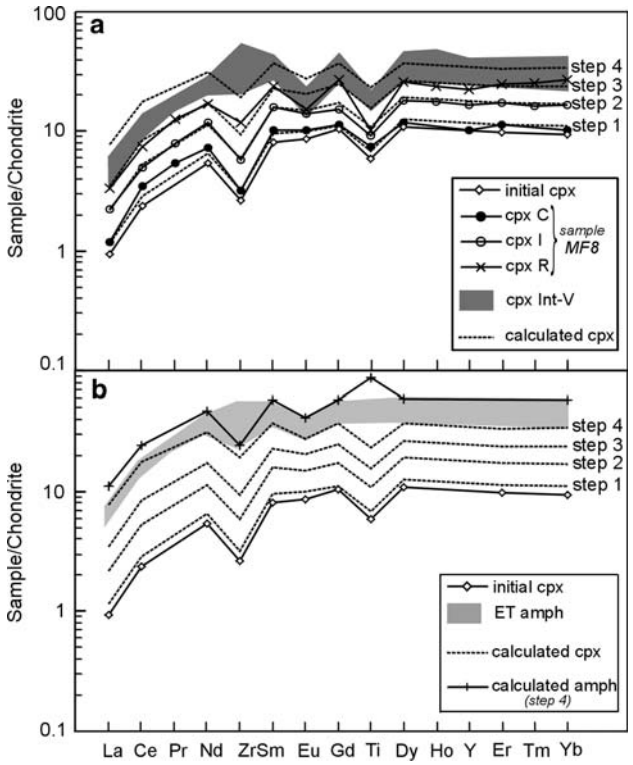

Fig. 9 **a** Chondrite-normalized REE abundances in clinopyroxenes calculated simulating an ''in situ fractionation'' process. The model consists of four steps of equilibrium cristallization [$C_L = C^0_L/(F + D–FD)$], where C_L and C^0_L are the concentrations of a trace element in the final and original liquid respectively, F is the remaining liquid fraction and D is the bulk distribution coefficient of crystallizing solid. As starting original liquid (C^0_L) in the first step (step 1) we have used the composition of liquid in equilibrium with the ''initial cpx'' (Fig. 8). Trace element crystal/liquid partition coefficients of clinopyroxene and plagioclase are from Suhr et al. (1998), crystal/liquid partition coefficients of amphibole are from Ionov et al. (2002). In all step we assume a crystallizing 70% cpx + 30% plag solid. Details about the single crystallization steps are: step 1, 20% of initial liquid ($F = 0.8$); step 2, 50% of remaining liquid ($F = 0.5$; i.e. 40% of the total liquid); step 3, 40% of remaining liquid ($F = 0.6$; i.e. ≈15% of the total liquid); step 4, 60% of remaining liquid ($F = 0.4$; i.e. 15% of the total liquid). After step 4, 90% of the total liquid has crystallized and the resulting bulk solid is constituted by 70% cpx + 30% plag; this implies about 3% crystallizing clinopyroxene, if 5% TMF is assumed. Computed clinopyroxenes have been calculated in equilibrium with the residual liquids of each step. Modelling results are compared with a representative core–intermediate–rim clinopyroxene profile from sample MF8. The *grey field* refers to the overall variation range defined by interstitial and vermicular clinopyroxenes. **b** Computed clinopyroxenes and ''initial cpx'' as in Fig. 9a. Computed amphibole has been calculated in equilibrium with the residual liquid of step 4. The *grey field* refers to the overall variation range defined by interstitial amphiboles from this study

opyroxene crystallized from the TMF, in agreement with the observed clinopyroxene modal amounts.

Modelling results are reported in Fig. 9a, which shows the trace element compositions of: (1) clinopyroxenes computed in equilibrium with the residual liquid of each crystallization step, (2) the ''initial clinopyroxene'', i.e. that in equilibrium with the starting liquid, (3) a representative core–intermediate–rim clinopyroxene profile from sample MF8 (Fig. 5), and (4) the variation range defined by interstitial and vermicular clinopyroxenes (grey field). This in situ fractional crystallization model reasonably simulates the progressive REE enrichment observed in ET clinopyroxenes. The composition of clinopyroxene core resembles computed clinopyroxene after 20% TM crystallization ($F = 0.8$, step 1), whereas clinopyroxenes calculated in step 2 and step 3 (up to 75% TMF crystallization) simulate REE, Zr and Ti concentrations of intermediate and rim analyses respectively, thus accounting for REE–Zr–Ti zoning observed in core–intermediate–rim profile. The REE enrichment recorded by the interstitial and vermicular clinopyroxenes is obtained after about 90% of (clinopyroxene + plagioclase) crystallization (step 4, see Fig. 9 caption). Step 4 clinopyroxene, in spite of similar M-HREE absolute concentrations, displays less marked LREE fractionation relative to vermicular clinopyroxenes. It is worth noting that step 4 clinopyroxene has been calculated assuming a bulk clinopyroxene-dominated crystallizing solid (70% cpx + 30% plag), and modelling results show that the trace element enrichment and LREE fractionation vary depending on the plagioclase/clinopyroxene proportions crystallizing during the single steps. Therefore, higher trace element enrichment coupled to lower La_N/Sm_N and pronounced Eu_N negative anomalies recorded by the vermicular grains could be related to a local fractionation effect resulting by a bulk plagioclase-dominated crystallizing solid.

The step crystallization model of Fig. 9 shows that the large part of clinopyroxene crystallization (core–rim profiles of large grains) can be explained in terms of in situ crystal fractionation. On the other hand, the proposed model, although reproducing the REE composition of interstitial and vermicular clinopyroxenes, fails to account for their Ti/REE and Zr/REE. More pronounced Ti negative anomalies in vermicular clinopyroxene, relative to computed step 3 and step 4 clinopyroxenes, are likely due to the concomitant precipitation of Fe–Ti oxides, which was not considered in the modelling. We will show in the following section that progressive Zr enrichment in interstitial and vermicular clinopyroxenes was presumably related to a melt/rock interaction process.

Melt/rock interaction: constraints from HFSE/REE fractionation

Zr enrichment relative to the REEs has been documented in zoned clinopyroxenes from both ophiolitic (Tribuzio et al. 1999) and oceanic (Ross and Elthon 1997; Coogan et al. 2000a, b; Gao et al. 2007) cumulates. Tribuzio et al. (1999)

found an extreme Zr enrichment in clinopyroxene rims and inferred that this was caused by the early precipitation of Zr-poor phases (i.e. clinopyroxene, plagioclase, apatite and Fe–Ti oxides), which increased Zr concentration in the residual liquid. Coogan et al. (2000a) showed that different processes can be invoked to explain positive Zr anomalies in clinopyroxene rims from oceanic gabbros, making a unique interpretation impossible. Zr enrichment beyond that expected by fractional crystallization was also documented in clinopyroxene rims from a Greenland gabbronorite (Bernstein 2006). Bernstein (2006) ascribed this geochemical signature to disequilibrium partitioning of Zr during rapid crystal growth (Shimizu 1981). In the ET troctolites, the evidence of very low TMF indicates rather slow cooling rate and efficient compaction and this argues against disequilibrium partitioning.

Coogan et al. (2000b), based on the evidence that Zr_N/Nd_N increase coupled to Mg# decrease occurs in a large part of intercumulus clinopyroxenes from MAR gabbros, inferred that the crystallization was largely controlled by metasomatism of exotic evolved melt migrating via reactive porous flow through the crystal mush. They used the assimilation and fractional crystallization equations (AFC; DePaolo 1981) to test that ''magmatic metasomatism'' is capable to produce the observed Zr_N/Nd_N zoning profile in clinopyroxenes. A similar approach was proposed by Gao et al. (2007) in a study on SWIR gabbros; they inferred that high Zr_N/La_N ratios in clinopyroxene rims can be simulated by an AFC process driven by clinopyroxene assimilation, with a variable modal proportion of crystallizing plagioclase and clinopyroxene.

Figure 10 shows the covariation of Zr_N and Nd_N in all clinopyroxenes from the ET troctolites together with computed clinopyroxene trends for fractional crystallization, equilibrium crystallization and the in situ fractionation model discussed above (details of modelling parameters are explained in Fig. 10 caption). As stated already, the in situ fractionation model match the compositional data for clinopyroxene core–rim profiles suggesting that this is the dominant mechanism (at least until 75% of TMF crystallization) to produce the observed REE and Zr variations (Figs. 9a, 10), whereas interstitial and vermicular grains diverge towards significant Zr enrichment.

Following Coogan et al. (2000b) and Gao et al. (2007), we used the AFC modelling to test whether a process of fractional crystallization and simultaneous assimilation is capable to produce the observed Zr enrichment in interstitial-vermicular clinopyroxenes. Input parameters are the initial melt composition, the ratio of the mass assimilated to the mass crystallized (Ma/Mc), the melt fraction remaining and the composition of the material assimilated (see Fig. 11 caption for modelling details). Results in terms of Yb_N and Ce_N/Sm_N versus Zr_N/Nd_N covariation trends in

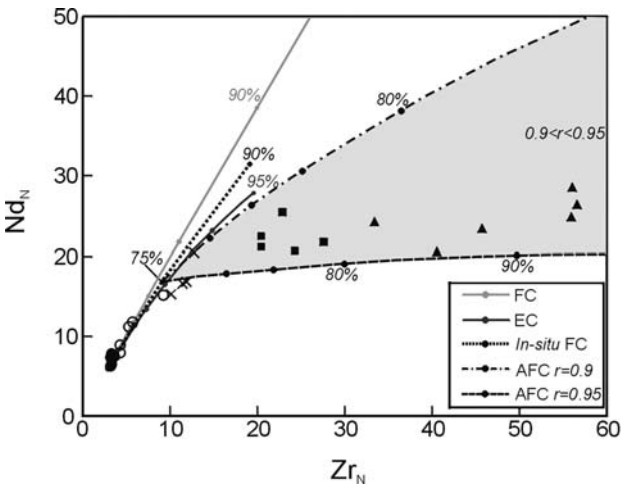

Fig. 10 Modelled covariation of Zr_N and Nd_N in clinopyroxene using: (1) fractional crystallization (*FC*), (2) equilibrium crystallization (*EC*), and (3) the in situ fractional crystallization step model of Fig. 9. Model trends were calculated assuming the initial melt as in the step model of Fig. 9, crystal/liquid partition coefficients from Suhr et al. (1998), and a bulk crystallized solid of 70% cpx + 30% plag. ET clinopyroxenes data are also reported (symbols as Fig. 3). The *grey field* is defined by AFC modelling trends computed assuming as starting liquid the evolved residual liquid after step 3 of in situ fractionation modelling, Ma = 100% olivine, a crystallizing bulk solid consisting of (10% cpx + 90% plag), and Ma/Mc = 0.9 and 0.95, respectively

clinopyroxene are given in Fig. 11, which also reports the ET clinopyroxene data. Calculations were performed assuming: (1) the initial melt as in the in situ fractionation model of Fig. 9, (2) different Ma/Mc (0.7, 0.9 and 0.95), (3) variable mode proportions of the crystallized minerals (see Fig. 11 caption). As discussed by Coogan et al. (2000b), the composition of assimilated material (Ma) is difficult to constrain and can be variable. Therefore, we used two different Ma compositions, i.e. 100% clinopyroxene (as proposed by Coogan et al. 2000b; Gao et al. 2007) and 100% olivine, this latter being the dominant cumulus minerals in the studied rocks.

Modelling results assuming clinopyroxene assimilation show that the crystallization trends fitting the observed Yb_N versus Zr_N/Nd_N variations (*trend2* and *trend3*; Fig. 11a) fail to preserve the LREE fractionation, resulting in much higher Ce_N/Sm_N ratios (Fig. 11b). On the other hand, if olivine assimilation is considered, the REE-Zr compositions of interstitial and vermicular clinopyroxenes can be reproduced assuming high Ma/Mc ratios (ranging 0.9–0.95, *trend7* and *trend8* of Fig. 11c, d) and a plagioclase-dominated mode of bulk crystallizing solid.

Coogan et al. (2000b) and Gao et al. (2007) used the AFC model to simulate the reactive porous flow migration of interstitial melt through a crystal mush. In the ET troctolites, anomalous Zr enrichments are only observed in very small (<400 μm) interstitial and vermicular clinopy-

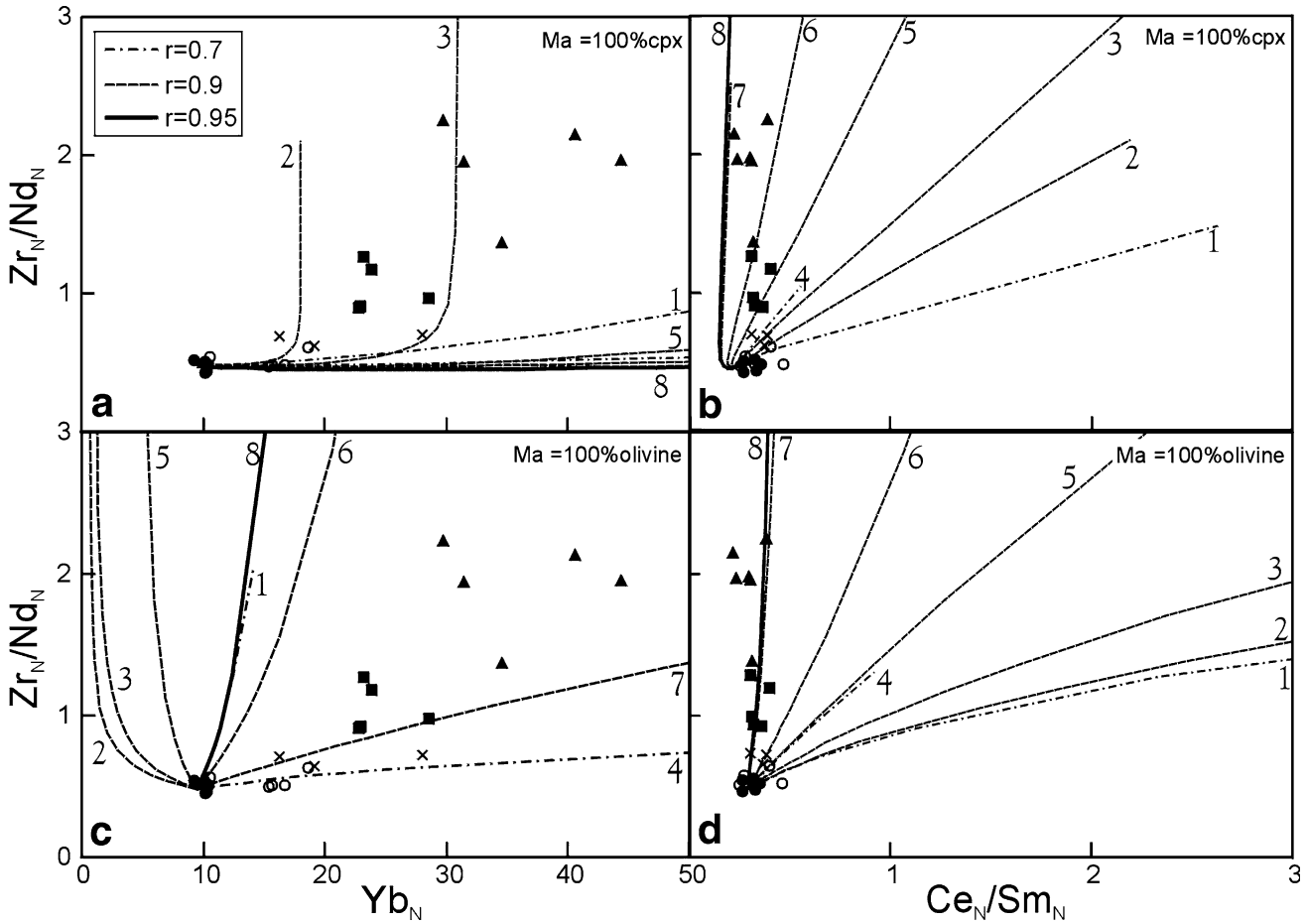

Fig. 11 **a** Zr_N/Nd_N versus Yb_N and **b** Zr_N/Nd_N versus Ce_N/Sm_N covariation in clinopyroxene computed by AFC modelling assuming Ma = 100% clinopyroxene (sample MF21 cpx1-C of eTable 2) and different Ma/Mc ratios (0.7, 0.9 and 0.95). Model trends were computed using the initial liquid composition as in the step model of Fig. 9, and partition coefficients from Suhr et al. (1998). Variable mode proportions of crystallized minerals were assumed: *1–2*: (70% cpx, 30% plag), *3*: (50% cpx, 50% plag), *4–5*: (30% cpx, 70% plag), *6*: (20% cpx, 80% plag), *7–8*: (10% cpx, 90% plag). ET clinopyroxenes data are also reported (symbols as Fig. 3). **c** Zr_N/Nd_N versus Yb_N and **d** Zr_N/Nd_N versus Ce_N/Sm_N covariation in clinopyroxene computed by AFC modelling assuming Ma = 100% olivine. The composition of assimilated olivine was calculated in equilibrium with the initial liquid as in the step model of Fig. 9 and using partition coefficients from Suhr et al. (1998). Modelling parameters are as in Fig. 11a, b

roxene grains which represent a very low late-stage melt fraction (reasonably <2%). At this final crystallization stage, it is likely that the low residual porosity inhibited large-scale melt migration. This suggests that other processes, rather than significant porous melt flux through the crystal mush, must be invoked to explain the observed Zr enrichment in clinopyroxene.

Textural observations show that interstitial and vermicular clinopyroxenes often display lobate contacts against cumulus olivine, indicative of interaction and partial dissolution by late stage interstitial liquids. Thus, a melt-rock interaction process involving olivine resorption could have occurred during the crystallization of final evolved liquid fractions (as inferred in AFC modelling of Fig. 11c, d), causing the observed Zr/REE fractionation. Moreover, we have shown in the previous paragraph that the crystallization of large clinopyroxene grains is accounted by in situ fractional crystallization of about 75% TMF. Based on these observations, we refined the AFC modelling of Fig. 11 using as starting melt the evolved residual liquid after step 3 of in situ fractionational crystallization, and again assuming high-Ma/Mc ratios and a plagioclase-dominated crystallizing mode (similar to *trend7* and *trend8* of Fig. 11c, d). Figure 10 shows that the Zr–Nd covariation of interstitial and vermicular clinopyroxenes plots within the compositional field defined by computed AFC trends at Ma/Mc ranging 0.9–0.95. Similar high Ma/Mc ratios were inferred by Coogan et al. (2000b), and could be related to slow cooling rates and/or limited melt migration through the crystal mush.

In summary, we infer that postcumulus crystallization in the ET troctolites was largely controlled by in situ fractional crystallization of trapped interstitial liquid rather then large-scale porous flow melt migration. Zr enrichment in late stage interstitial and vermicular clinopyroxenes was likely related to small-scale migration and interaction between residual evolved low melt fractions and the olivine cumulus matrix.

Origin of interstitial pargasitic amphibole in primitive cumulates

The occurrence of pargasitic amphiboles is a recurrent feature in MORB-type gabbroic rocks from oceanic ridge environments (Gillis 1996; Cortesogno et al. 2000; Gillis and Meyer 2001; Coogan et al. 2001) and ophiolitic settings (Tribuzio et al. 2000). Two main hypotesis have been proposed for its origin: (1) hydrothermal, resulting from reactions between magmatic minerals (plagioclase and clinopyroxene) and oceanic fluids (Campbell et al. 1988; Michard 1989; Gillis and Meyer 2001), (2) magmatic, related to crystallization of enriched intercumulus melt during final stage of cumulus body solidification (Gillis 1996; Tribuzio et al. 2000; Gillis and Meyer 2001; Coogan et al. 2001).

In the ET troctolites, pargasitic amphiboles occur as thin rim around spinel, and associated to vermicular clinopyroxene. High absolute concentrations of incompatible elements like Nb, Zr and REE suggest that they crystallized from igneous liquids (rather than at subsolidus conditions by interaction with seawater-derived fluids), similar to previous studies on Ti-rich pargasites in olivine cumulates (Tribuzio et al. 2000; Gillis and Meyer 2001; Coogan et al. 2001). Given a magmatic origin, it is a matter of debate whether amphibole in primitive MORB-type cumulates can derive from closed-system crystallization, or an external H_2O-rich component needs to be invoked (open-system crystallization). The critical question is that MORBs have very low H_2O concentrations (0.1–0.4 wt.% for most MORB; Michael 1988; Sobolev and Chaussidon 1996; Danyushevsky et al. 2000) whereas a minimum H_2O amount of 2–4 wt.% in the melt is needed to stabilize amphibole (Rutherford et al. 1985; Sisson and Grove 1993; Sato et al. 1999). Previous studies inferred that assuming a starting MORB liquid composition with a H_2O content ranging 0.1–0.20 wt.%, 90–95% fractional crystallization driven by anhydrous minerals would be required to yield a melt with enough H_2O (2–6 wt.%) to stabilize amphibole (Tribuzio et al. 2000; Gillis and Meyer 2001). Such process has been inferred by Gillis and Meyer (2001), who proposed a closed-system fractional crystallization model able to obtain amphibole appearance after 90% of original melt crystallization, and to reproduce compositions comparable to those of amphiboles from oceanic cumulates (Hess Deep, MARK and Hole 735B). On the other hand, Tribuzio et al. (2000) argued that LREE enrichment in pargasites from Northern Apennine ophiolitic gabbros (see Figs. 6b, 7) is inconsistent with closed-system trapped melt crystallization, rather it involved the percolation of an external, highly evolved (H_2O-LREE-rich), interstitial melt.

Pargasitic amphiboles in the ET troctolites are characterized by compositional decoupling between major and trace element contents. They display relatively high Mg# (0.86–0.89) in spite of high absolute Nb, Zr and REE concentrations (50–60 × C1) (Fig. 6b). As already argued for the interstitial clinopyroxene, this major-trace element decoupling indicates that amphibole crystallized from an evolved residual interstitial melt which was buffered in terms of major elements (e.g. Mg value) by the cumulus olivine matrix. However, in spite of marked trace element enrichment, amphiboles, similar to vermicular clinopyroxenes, preserve significant LREE fractionation (La_N/Sm_N = 0.11–0.15) (Fig. 7), and this argues against the involvement of a LREE-rich externally derived component. In Fig. 9b, we reported the REE–Zr–Ti composition of amphibole computed after 90% crystallization (step 4) of a small (5%) TMF (according to the in situ fractional crystallization model), compared to the overall variation range defined by ET amphiboles. As previously discussed for the interstitial and vermicular clinopyroxenes, the in situ fractional crystallization model can reproduce the REE spectra of ET amphiboles, but it is unable to simulate the Zr and Ti behaviour. As inferred for clinopyroxenes, lower Ti content in amphiboles relative to calculated composition are probably due to the concomitant precipitation of Fe–Ti oxides, which was not considered in the modelling. Amphiboles also show variable Zr/REE fractionation, and generally higher Zr abundances relative to computed step 4 amphibole. It is remarkable that amphiboles occurs in very thin interstitial grains (usually <60 μm), often in textural equilibrium with vermicular clinopyroxene, thus representing the same late crystallization stage. High Zr contents in amphiboles could be therefore related to the Zr-enriched signature of late-stage low melt fractions, acquired by melt/rock interaction via olivine dissolution (see discussion above). Amph/cpx trace element distribution coefficients calculated for vermicular grains overall reflect equilibrium partitioning, thus supporting this hypothesis; it is however unclear the reason why the highest Zr enrichments are observed in clinopyroxene, resulting in amph/cpx coefficients for Zr slightly lower than expected. The involvement of very low melt fractions, representing the final 5–10% of TMF crystallization, would also account for H_2O saturation, needed to stabilize amphibole.

Conclusions

Combined microtextural data and in situ trace element mineral analyses reveal that interstitial melt crystallization occurred during the latest stages of solidification of MORB-type primitive olivine cumulates intruded in the ET mantle peridotites (Voltri Massif). Peculiar chemical features in interstitial clinopyroxenes and Ti-rich pargasites, namely their significant trace element enrichment at almost constant LREE fractionation, argue against the infiltration of exotic highly evolved melts and indicate that interstitial minerals were dominantly related to closed-system trapped melt crystallization. Geochemical modelling shows that low amounts (<5%) of trapped melt crystallization are sufficient to produce REE enrichments similar to those observed in clinopyroxenes. Although the progressive increase in overall trace element abundances (from core to rim of large clinopyroxene grains) is accounted by an ''in situ'' fractional crystallization process, Zr enrichment in thin (<400 μm) interstitial and vermicular clinopyroxenes was likely related to small-scale migration and interaction between residual, evolved, low melt fractions and the olivine cumulus matrix.

In the ET troctolites, the evidence of low TMF argue against large-scale residual melt migration, this latter being controlled by porosity and permeability of the crystal mush, and indicates that the compaction was very efficient. This could have been favoured by the interplay of different factors, i.e. slow cooling rates and low thermal gradients (as inferred by Meyer et al. 1989 in very slow spreading ridge gabbros) and synkinematic deformation (Natland and Dick 2001). Structural and petrologic investigations on the ET cumulates have shown that they represent pre-oceanic rift gabbroic intrusions (Sm/Nd crystallization age of 180 ± 14 Ma; Rampone et al. 2005) which crystallized at moderate pressures (3–5 kbar) within extending subcontinental lithospheric mantle (Borghini et al. 2007). Moreover, field and geochemical evidence (Borghini et al. 2007) has revealed that the host mantle peridotites experienced diffuse impregnation by depleted melts before the intrusion of discrete MORB-type gabbroic bodies, and this impregnation stage likely caused reheating of the shallow lithospheric mantle. This implies that the country peridotites were still rather hot (1,100–1,200°C) when intruded by parental melts to the cumulate body, as suggested by the diffuse (never sharp) style of peridotite-cumulate contacts. Therefore, slow cooling rates in the cumulates were favoured by low thermal gradients relative to the country rocks and by rather deep-seated emplacement. Deformation during solidification (as proposed by Natland and Dick 2001) could have further enhanced squeezing out of the residual evolved interstitial liquids, although differentiated veins are not observed in the field. In this context, it is remarkable that the ET troctolites are primitive cumulates in primary intrusive contacts with mantle peridotites, and they could represent the base of a stack of cumulates from which differentiated melts migrated upwards and crystallized at shallower lithospheric environments (not observed in the field). The subsequent, postmagmatic, history of the ET cumulates was governed by extension–related cooling and uplift (Borghini et at. 2007), and this could have prevented significant postcumulus trace element redistribution in minerals by diffusion, as testified by preservation of systematic trace element zoning in clinopyroxene.

Acknowledgements We acknowledge A. Zanetti (Pavia) and L. Negretti (Genova) for assistance with the LAM-ICP-MS and EDS analyses. M. Godard (Montpellier) and M. Mazzucchelli (Modena) are greatly thanked for providing ICP–MS and XRF bulk-rock analyses. Reviews from D. Ionov and an anonymous referee are gratefully acknowledged for constructive criticisms and suggestions, which improved an early version of the paper. We also thank R. Tribuzio for stimulating discussion. We acknowledge funding by the University of Genova and Italian PRIN-COFIN to the project ''The role of melt-peridotite interaction in the modification and evolution of the lithospheric mantle''.

References

Anders E, Ebihara M (1982) Solar system abundances of the elements, Geochim Cosmochim Acta 46:2363–2380

Barnes SJ (1986) The effect of trapped liquid crystallization on cumulus mineral compositions in layered intrusions. Contrib Mineral Petrol 93:524–531

Bedard JH (1994) A procedure for calculating the equilibrium distribution of trace elements among the minerals of cumulate rocks, and the concentration of trace elements in coexisting liquids. Chem Geol 118:143–153

Bedard JH (2001) Parental magmas of the Nain plutonic suite anorthosites and mafic cumulates: a trace element modelling approach. Contrib Mineral Petrol 141:747–771

Bender JF, Hodges FN, Bence AE (1978) Petrogenesis of basalts from the project FAMOUS area: experimental study from 0 to 15 Kbar. Earth Planet Sci Lett 41:277–302

Bernstein S (2006) In situ fractional crystallization of a mafic pluton: microanalytical study of a Paleogene gabbronorite plug in East Greenland. Lithos 92:222–237

Borghini G, Rampone E, Piccardo GB, Crispini L, De Ferrari R, Godard M (2007) Origin and emplacement of ultramafic-mafic intrusions in the Erro–Tobbio mantle peridotites (Ligurian Alps, Italy). Lithos 94:210–229

Campbell AC, Palmer MR, Kinkhammer GP, Bowers TS, Edmond JM, Lawrence JR, Casey JF, Thompson G, Humpris S, Rona P, Karson JA (1988) Chemistry of hot springs on the Mid-Atlantic Ridge. Nature 335:514–519

Cawthorn RG, Sander BK, Jones IM (1992) Evidence for the trapped liquid shift effect in the Mount Ayliff Intrusion, South Africa. Contrib Mineral Petrol 111:194–202

Cawthorn RG (1996) Models for incompatible trace element abundances in cumulus minerals and their application to plagioclase and pyroxenes in the Bushveld Complex. Contrib Mineral Petrol 123:109–115

Chalokwu CI, Grant NK (1990) Petrology of the partrige river intrusion, Duluth complex, Minnesota: 1. Relationships between

mineral compositions, density and trapped liquid abundance. J Petrol 31:265–293
Charlier B, Auwera JV, Duchesne JC (2005) Geochemistry of cumulates from the Bjerkreim-Sokndal layered intrusion (S. Norway) Part II. REE and the trapped liquid fraction. Lithos 83:255–276
Cherniak DJ (2003) REE diffusion in feldspar. Chem Geol 193:25–41
Claeson DT, Meurer WP (2004) Fractional crystallization of hydrous basaltic ''arc-type'' magmas and the formation of amphibole-bearing gabbroic cumulates. Contrib Mineral Petrol 147:288–304
Coogan LA, Kempton PD, Saunders AD, Norry MJ (2000a) Melt aggregation within the crust beneath the Mid-Atlantic Ridge: evidence from plagioclase and clinopyroxene major and trace element compositions. Earth Planet Sci Lett 176:245–257
Coogan LA, Saunders AD, Kempton PD, Norry MJ (2000b) Evidence from oceanic gabbros for porous melt migration within a crystal mush beneath the Mid-Atlantic Ridge. Geochem Geophys Geosys 1 paper number 2000GC000072
Coogan LA, Wilson RN, Gillis KM, MacLeod CJ (2001) Near-solidus evolution of oceanic gabbros: insights from amphibole geochemistry. Geochim Cosmochim Acta 65:4339–4357
Cortesogno L, Gaggero L, Zanetti A (2000) Rare earth and trace elements in igneous and high-temperature metamorphic minerals of oceanic gabbros (MARK area, Mid-Atlantic Ridge). Contrib Mineral Petrol 139:373–393
Danyushevsky LV, Eggins SM, Falloon TJ, Christie DM (2000) H_2O abundance in depleted to moderately enriched Mid-ocean Ridge magmas; Part I: incompatible behaviour, implications for mantle storage, and origin of regional variations. J Petrol 41:1329–1364
DePaolo DJ (1981) Trace element and isotopic effects of combined wallrock assimilation and fractional crystallization. Earth Planet Sci Lett 53:189–202
Elthon D, Stewart M, Ross KD (1992) Compositional trends of minerals in oceanic cumulates. J Geophys Res 97:5-189–5-199
Gao Y, Hoefs J, Hellebrand E, von der Handt A, Snow JE (2007) Trace element zoning in pyroxenes from ODP Hole 735B gabbros: diffuse exchange or synkinematic crystal fractionation? Contrib Mineral Petrol 153:429–442
Gillis KM (1996) Rare earth element constraints on the origin of amphibole in gabbroic rock from site 894, Hess Deep. In: Mevel C, Gillis KM, Allan JF, Meyer PS (eds) Ocean Drilling program scientific results, vol 147. College Station, TX, USA, pp 59–75
Gillis KM, Meyer PS (2001) Metasomatism of oceanic gabbros by late stage melts and hydrothermal fluids: evidence from the rare earth element composition of amphiboles. Geophys Geochem Geosys 2, paper number 2000GC000087
Godard M, Jousselin D, Bodinier J-L (2000) Relationships between geochemistry and structure beneath a paleo-spreading centre: a study of the mantle section in the Oman ophiolite. Earth Planet Sci Lett 180:133–148
Green DH, Falloon TJ, Eggins SM, Yaxley GM (2001) Primary magmas and mantle temperatures. Eur J Mineral 13:437–451
Hofmann AW (1988) Chemical differentiation of the earth: the relationships between mantle, continental crust and oceanic crust. Earth Planet Sci Lett 90:297–314
Ionov DA, Savoyant L, Dupuy C (1992) Application of the ICP-MS technique to trace element analysis of peridotites and their minerals. Geostandards Newsl 16:311–315
Ionov DA, Bodinier JL, Mukasa SB, Zanetti A (2002) Mechanisms and sources of mantle metasomatism: major and trace element compositions of peridotite xenolites from Spitbergen in the context of numerical modelling. J Petrol 43:2219–2259
Leake BE (1997) Nomenclature of amphiboles: report of the subcommittee on amphiboles of the international mineralogical association, commission on new minerals and mineral names. Am Mineral 82:1019–1037
Mathez EA (1995) Magmatic metasomatism and formation of the Merensky reef, Bushveld Complex. Contrib Mineral Petrol 119:277–286
Meurer WP, Claeson DT (2002) Evolution of crystallizing interstitial liquid in an arc-related cumulate determined by LA ICP-MS mapping of a large amphibole oikocryst. J Petrol 43:607–629
Meyer PS, Dick HJB, Thomson G (1989) Cumulates gabbro from the Southwest Indian Ridge, 54° S–7°13′ E: implication for magmatic processes at a slow spreading ridge. Contrib Mineral Petrol 103:44–63
Michael PJ (1988) The concentration, behaviour and storage of H_2O in the suboceanic upper mantle: implications for mantle metasomatism. Geochim Cosmochim Acta 52:555–566
Michard A (1989) Rare earth element systematics in hydrothermal fluids. Geochim Cosmochim Acta 53:745–750
Natland JH, Meyer PS, Dick HJB, Bloomer SH (1991) Magmatic oxides and sulfides in gabbroic rocks from Hole 735B and the later development of the liquid line of descent. In: Von Herzen RP, Robinson PT, et al (eds) Proceedings of the ODP, science results, vol 118. Ocean Drilling Program, College Station, TX, pp 75–111
Natland JH, Dick HJB (2001) Formation of the lower ocean crust and the crystallization of gabbroic cumulates at a very slowly spreading ridge. J Volcanology Geothermal Res 110:191–233
Rampone E, Hofmann AW, Raczek I (1998) Isotopic contrasts within the Internal Liguride ophiolite (N. Italy): the lack of a genetic mantle-crust link. Earth Planet Sci Lett 163:175–189
Rampone E, Piccardo GB, Romairone A, Raczek I, Abouchami W, Hofmann AW (2005) Mantle-crust relations in embryonic slow spreading ocean basins: insights from the Ligurian and Corsica ophiolites. Geophys Res Abstract EGU05-A-07883
Ross K, Elthon D (1997) Cumulus and postcumulus crystallization in the ocean crust: major- and trace-element geochemistry of leg 153 gabbroic rocks. In: Karson JA, Cannat M, Millet DJ, Elthon D (eds) Proceedings of the Ocean Drilling Program, scientific results, vol 153. Ocean Drilling Program, College Station, TX, pp 333–350
Rutherford MJ, Sigurdsson H, Carey S, Davis A (1985) The May 18, 1980, eruption of Mount St. Helens, 1, Melt composition and experimental phase equilibria. J Geophys Res 90:2929–2947
Sato H, Nakada S, Fujii T, Nakamura M, Suzuki-Kamata K (1999) Groundmass pargasite in the 1991–1995 dacite of Unzen volcano: phase stability experiments and volcanological implications. J Volcanol Geotherm Res 89:197–212
Shimizu N (1981) Traceelement incorporation into growing augite phenocryst. Nature 289:575-577
Sisson TW, Grove TL (1993) Temperatures and H2O contents of low-Mg high-alumina basalts. Contrib Mineral Petrol 113:167–184
Sobolev AV, Chaussidon M (1996) H2O concentrations in primary melts from supra-subduction zones and mid-ocean ridges: implications for H_2O storage and recycling in the mantle. Earth Planet Sci Lett 137:45–55
Suhr G, Seck HS, Shimizu N, Gunther D, Jenner G (1998) Circulation of refractory melts in the lowermost oceanic crust: evidence from a trace element study of dunite-hosted clinopyroxenes in the Bay of Islands Ophiolite. Contrib Mineral Petrol 122:387–405
Tiepolo M, Bottazzi P, Palenzona M, Vannucci R (2003) A laser probe coupled with ICP-double-focusing sector-field mass spectometer for in situ analyses of geological samples and U–Pb dating of zircon. Can Mineral 41:259–272
Tribuzio R, Tiepolo M, Vannucci R, Bottazzi P (1999) Trace element distribution within the olivine-bearing gabbros from the Northern Apennine ophiolites (Italy): evidence for post-cumulus crystallization in MOR-type gabbroic rocks. Contrib Mineral Petrol 134:123–133

Tribuzio R, Tiepolo M, Thirlwall MF (2000) Origin of titanian pargasite in gabbroic rocks from the Northern Apennine ophiolites (Italy): insights into the late-magmatic evolution of a MOR-type intrusive sequence. Earth Planet Sci Lett 176:281–293

Vaggelli G, Olmi F, Conticelli S (1999) Quantitative electron microprobe analysis of reference silicate mineral and glass samples. Acta Vulcanologica 11(2):297–303

Van Orman JA, Grove TL, Shimizu N (2001) Rare earth element diffusion in diopside: influence of temperature, pressure, and ionic radius, and an elastic model for diffusion in silicates. Contrib Mineral Petrol 141:687–703

Walter MJ, Presnall DC (1994) Melting behaviour of simplified lherzolite in the system CaO–MgO–Al_2O_3–SiO_2–-Na_2O from 7 to 35 kbar. J Petrol 35:329–359